Langmuir

Article

pubs.acs.org/Langmuir

S-Shaped Conformation of the Quaterthiophene Molecular Backbone in Two-Dimensional Bisterpyridine-Derivative Self-Assembled Nanoarchitecture

Yann Kervella,[†] Ekaterina Shilova,[‡] Sylvain Latil,[§] Bruno Jousselme,[†,∥] and Fabien Silly*[,⊥]

[†]CEA Grenoble INAC/SPrAM UMR 5819 CEA - CNRS - Univ. J. Fourier-Grenoble 1, LEMOH, 17 Rue des Martyrs, 38054 Grenoble Cedex 9, Grenoble, France

[‡]Ajelis, 86 rue de Paris, F-94100 Orsay, France

[§]MSIN, SPEC, CEA, CNRS, [∥]LICSEN, NIMBE, CEA, IRAMIS, CNRS, and [⊥]TITANS, SPEC, CEA, CNRS, Université Paris-Saclay, CEA Saclay F-91191 Gif sur Yvette, France

Supporting Information

ABSTRACT: The conformation and the two-dimensional self-assembly of 4′-(3′,4″-dihexyloxy-5,2′:5′,2″:5″,2‴-quaterthien-2,5‴-diyl)-bis(2,2′:6′,2″-terpyridine) molecules are theoretically and experimentally investigated. This molecular building block forms a hydrogen-bonded chiral supramolecular nanoarchitecture on graphite at the solid/liquid interface. Scanning tunneling microscopy (STM) shows that the molecule adopts an S-shaped conformation in this structure. DFTB+ calculations reveal that this conformation is not the lowest-energy conformation. The molecular nanoarchitecture appears to be stabilized by hydrogen bonding as well as van der Waals interactions. I-, L-, and D-shaped molecular conformations are, however, locally observed at the domain boundary, but these conformations do not self-assemble into organized 2D structures.

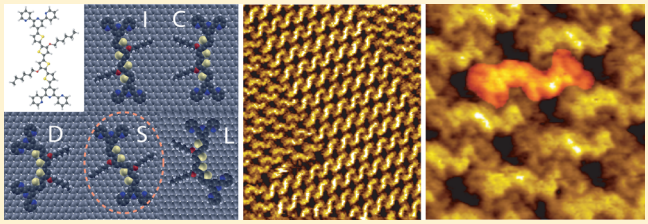

INTRODUCTION

Engineering novel organic/inorganic interfaces thought the self-assembly of functionalized molecules[1−11] is attracting an enormous amount of research interest due to its expected applications in nanotechnology.[12−14] The electronic properties of a self-assembled organic or hybrid layer can be drastically affected by the organization of its building blocks at the interface with a conductive surface.[15,16] Controlling the arrangement of the building nanoblock at the nanoscale is therefore a key parameter governing the properties of the interface. Hydrogen bonding is a particularly appealing interaction governing molecular self-assembly due to the strength, the high selectivity, and the directionality of this binding.[17−27] Carboxylic groups can be used to strengthen molecular self-assembly because these substituents are expected to lead to the formation of double hydrogen bonds (O−H···O) between neighboring molecules. This strategy has been successfully used to achieve the formation of self-assembled porous and compact nanoachitectures.[28−31] An alternative consists of functionalizing the molecular skeleton with pyridine units instead of carboxylic groups. Pyridine is also expected to drive molecular self-assembly through the formation of double hydrogen bonds (C−H···N) between neighboring molecules. Intense effort has recently been devoted to the synthesis of pyridine-based molecular building blocks.[32,33] Hydrogen-bonded densely packed and porous nanoarchitectures have been engineered using pyridine-based molecular building blocks.[34,35] The review of Wild et al. summarized the recent research effort in synthesizing π-conjugated 2,2′:6′,2″-terpyridine ligands for application in the fields of supramolecular and coordination chemistry and materials science.[32] The pyridine groups are expected to drive molecular self-assembly through hydrogen bonding or metal coordination whereas the spacer unit is carrying the electronic properties or the active part of the molecular building block. Among the possible spacer units, oligothiophenes are very interesting because their chemistry is now well known to tune their electronic, optical, and redox properties for applications in organic electronics.[36]

A compound mixing two flat conjugated system based on bisterpyridines and quaterthiophene is therefore a promising building block for engineering highly organized self-assembled organic films. However, the pyridine and thiophene units can rotate along their C−C axis in the terpyridine and the quaterthiophene groups. Molecules can adopt different conformations once adsorbed on surfaces.[37−39] Yokoyama et al. investigated the *cis* and *trans* conformations of single thiophene derivatives using scanning tunneling microscopy,[40] but they were not able to resolve the backbone structure of the molecule. This is essential to assessing individual molecular conformation because their electronic properties are governed by intramolecular π-conjugation that depends on the torsion

Received: September 4, 2015
Published: December 1, 2015

DOI: 10.1021/acs.langmuir.5b03949
Langmuir 2015, 31, 13420−13425

angle between neighboring thiophene cycles.[41−44] In addition, it is unclear if the flexibility of the molecular skeleton can lead to the formation of ordered nanoarchitectures.

In this paper, we synthesized a new organic building block with a quaterthiophene spacer functionalized in positions α with two terpyridine groups (4T-bisterpy) (Figure 1). This

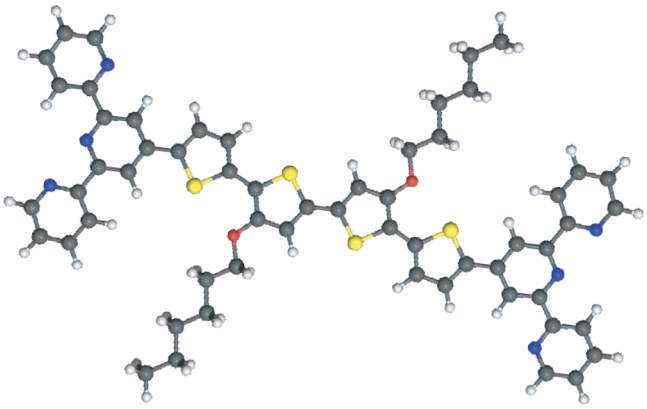

Figure 1. Scheme of the 4T-bisterpy molecule ($C_{58}H_{52}N_6O_2S_4$). Carbon atoms are gray, oxygen atoms are red, nitrogen atoms are blue, hydrogen atoms are white, and sulfur atoms are yellow.

compound can adopt five conformational structures. Scanning tunneling microscopy (STM) was used to investigate the self-assembly of this compound at the 1-phenyloctane/graphite interface. STM reveals that the molecules self-assembled into a two-dimensional chiral nanoarchitecture based on a single molecular conformational structure.

EXPERIMENTAL SECTION

The molecule was synthesized according to the procedure described in the Supporting Information. Nearly saturated solutions of 4T-bisterpy (Figure 1) in 1-phenyloctane (98%, Aldrich) were prepared (concentration of 10^{-5} mol/L). A droplet of this solution was then deposited on a graphite substrate. STM imaging of the samples was performed at the liquid/solid interface[28,45−48] using a Pico-SPM (Molecular Imaging, Agilent Technology) scanning tunneling microscope. Cut Pt/Ir tips were used to obtain constant-current images at room temperature with a bias voltage applied to the sample. STM images were processed and analyzed using the FabViewer application.[49]

RESULTS AND DISCUSSION

Calculation of Molecular Conformational Energies. The chemical structure of 4T-bisterpy is presented in Figure 1. Depending on the orientation of the thiophene units, the 4T-bisterpy molecule can adopt five flat structural conformations as represented in Table 1. We used density functional tight-binding calculations, using the DFTB+ numerical package calculations, to estimate the energy of the five possible molecular conformations and their corresponding adsorption energy on a honeycomb graphitic sheet. The results are presented in Table 1 and Table 1 in Supporting Information.

The molecularly straight I shape has the lowest conformational energy (−4081.153 eV), followed by the C shape (−4081.123 eV). Then the S-shaped and L-shaped conformation have nearly the same energy, −4081.105 and −4081.103 eV, respectively. The L and D shapes have the two highest conformational energies. In conformations I and C, which present lower energies, S···O intramolecular interactions

Table 1. Scheme, Conformal Energy in the Gas Phase (E_{gas}), and Adhesion Energy (E_{adh}) per Molecule of the Five Molecular Conformations (Molecules Are Represented without Their Alkyl Chains)[a]

Scheme	Conformation	E_{Gas} (eV)	E_{Adh} (eV)	Δ_{eV}
	I	-4081.153	-5.021	0
	C	-4081.123	-5.017	+0.033
	S	-4081.105	-5.006	+0.063
	L	-4081.103	-4.876	+0.195
	D	-4081.079	-4.731	+0.364

[a]The surface energy of the graphitic sheet is −18 897.169189 eV. Δ_{eV} corresponds to the molecular total energy difference with respect to that of the I configuration.

between the oxygen of hexyloxy chains and the sulfur of an adjacent thiophene stabilize these two structures as previously reported in EDOT oligomers.[50] These interactions are not present in structures D and S, and only one is observed in the L conformation. Once the molecules are adsorbed on the graphitic substrate, calculations (E_{adh} in Table 1) show that the conformations can be categorized into two groups, i.e., a low-energy conformational group (I, C, and S conformations) and a high-energy conformational groups (L and D). The energy difference between the S and L shapes is significant once molecules are adsorbed on the graphite surface.

Molecular Conformation on the Surface. The large-scale STM images reveal that 4T-bisterpy self-assembles into large domains at the 1-phenyloctane/graphite interface (Figure 2). The typical domain size is 1000 ± 200 nm^2. In Figure 3, the high-resolution STM image shows the domain boundary between two enantiomeric self-assembled nanoarchitectures. The domain boundary is highlighted by white arrows in the image. The building blocks of the two domains are two 4T-bisterpy enantiomers. These enantiomers have been colored in orange as a guide for the eyes in Figure 3. Intramolecular features corresponding to the integrated density of states of the molecule appear distinctly in the high-resolution STM image. In particular, the structural conformation of the molecular backbone is clearly resolved. The molecules adopt the S structure in the organic layer. The two molecular enantiomers can be observed in Figure 3. The unit cell is represented by dotted lines in the STM image. The unit cell is not strictly identical in neighboring domains, i.e., the flexibility of intermolecular binding and molecular conformation affects the unit cell of the domains. The network unit cell of this chiral structure is, however, a parallelogram with 1.9 ± 0.2 and 1.7 ± 0.2 nm unit cell constants and an angle of 80 ± 5° between the axes. Each chiral domain is based on a single enantiomer. Rectangular cavities, ∼1.0 × 0.7 nm^2, are formed in this nanoarchitecture above to terpyridine units of the molecules (dark area in the STM images, Figure 3). The model of the organic nanoarchitecture is presented in Figure 3b.

DOI: 10.1021/acs.langmuir.5b03949
Langmuir 2015, 31, 13420−13425

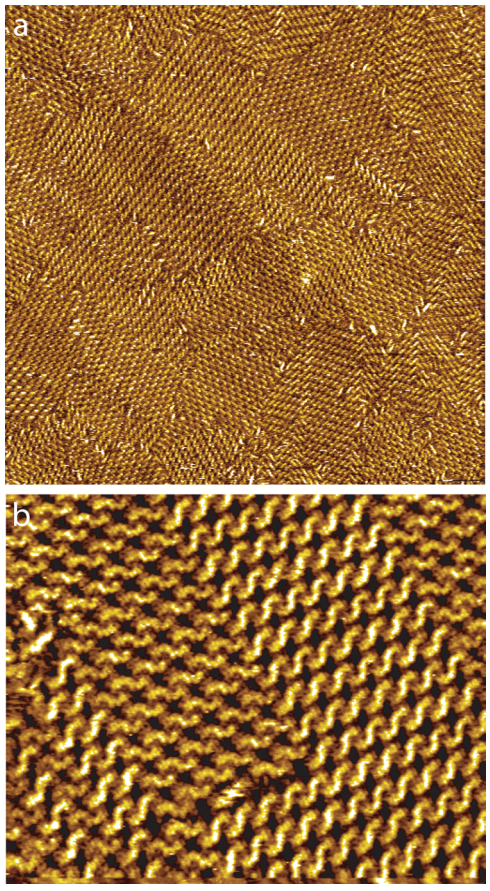

Figure 2. Large-scale STM images of the 4T-bisterpy self-assembled nanoarchitecture on graphite: (a) 155 × 155 nm^2 and (b) 30 × 25 nm^2, V_s = 0.40 V, and I_t = 9 pA.

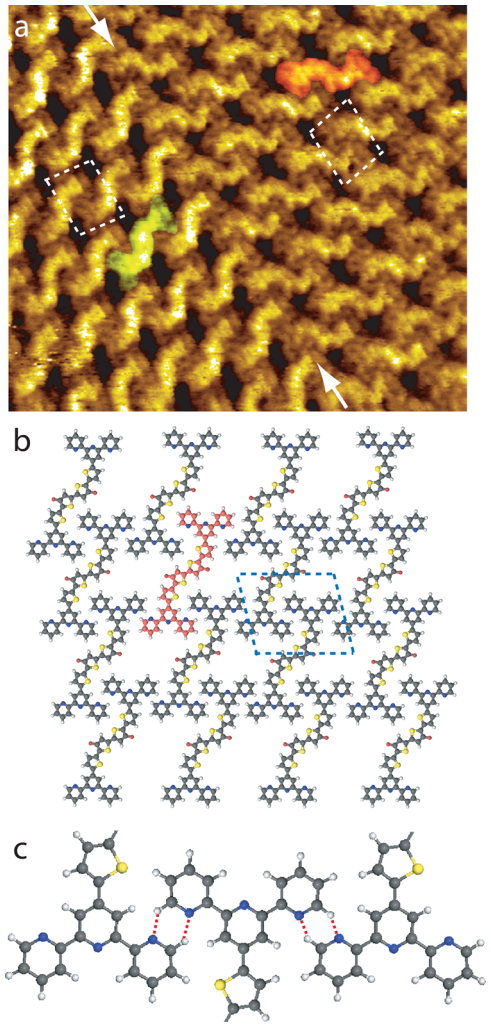

Figure 3. (a) High-resolution STM images of 4T-bisterpy chiral self-assembly: 15 × 13 nm^2, V_s = 0.40 V, and I_t = 9 pA. The two molecular enantiomers can be observed (orange and green). (b) Model of the nanoarchitecture. The parallelogram unit cells of the chiral domains are represented by dotted white (a) and blue lines (b). (Molecules are represented without their alkyl chains). (c) Scheme of intermolecular bonding. N···H−C bonds are represented by dotted red lines.

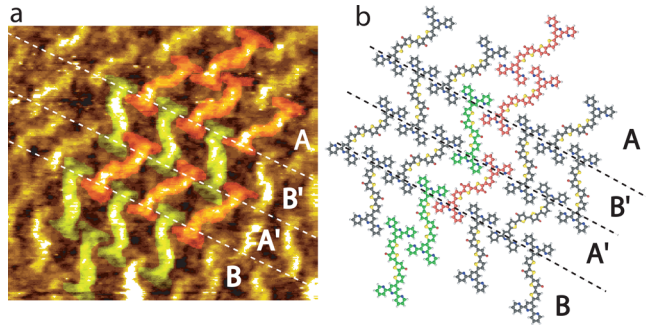

Figure 4. (a) STM images of a multiple domain boundary, 11 × 9 nm^2; V_s = 0.70 V and I_t = 10 pA. The two enantiomers have been colored in green and red. (b) Model (molecules are represented without their alkyl chains).

Organic domains are based on a single molecular enantiomer. The alternation of enantiomer rows can, however, be locally observed at the domain boundary (Figure 4). Careful analysis of the STM images reveals that at the domain boundary, rows of molecular enantiomers (B′ and A′) can be separating domains (A and B), as shown in Figure 4. However, we never observed a sequence larger than four rows of different enantiomers on the surface. This sequence is shown in Figure 4 (A-B′-A′-B). Because long-range ordering is not achieved with two enantiomers, it appears more appropriate to talk of the domain boundary instead of the network for this structure.

Hoster et al. has simulated intermolecular interactions in the case of bis(terpyridine)-based compounds' self-assembly.[51] Their calculations show that the two intermolecular bindings are favored when pyridine orientation allows C−H···N bonds between neighboring molecules. The organic nanoarchitecture in Figure 3 appears to be stabilized by double N···H−C hydrogen bonds between molecular pyridine rings in terpyridine. Surprisingly, the molecular building blocks adopt an S shape in the network. The other conformations can be seen locally only at the domain boundary, as shown in Figure 5. This is particularly puzzling because most of the experimental observations report on the self-assembly of molecular thiophene chains adopting a straight conformation.[52−56] The self-assembly of twisted conformations was rarely observed.[57] The STM images show that the molecule adopts the S conformation exclusively in the 2D self-assembled nanoarchitecture. The other molecular conformations represent less than 1% of the molecules. The I, L, and D conformations can be observed in Figure 5a−c, respectively. The C

DOI: 10.1021/acs.langmuir.5b03949
Langmuir 2015, 31, 13420−13425

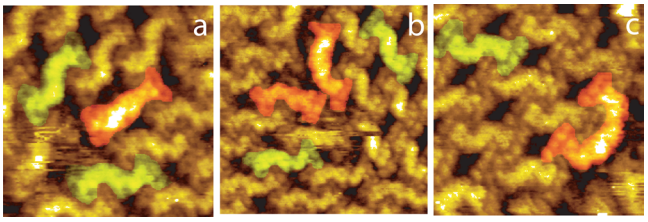

Figure 5. STM images of the molecular domain boundary. Molecules adopting the S conformation in the domain have been colored in green, and molecules adopting other conformations have been colored in orange. (a) I-shape conformation, 7 × 7 nm^2; (b) L-shape conformation, 9 × 9 nm^2; (c) D-shape conformation, 7 × 7 nm^2; V_s = 0.40 V and I_t = 9 pA.

conformation was not observed, but we do not rule out that it cannot exist locally.

The calculations show that the I- and C-shaped molecules have lower conformal energy (Table 1). Therefore, the S structure should be less favorable. However, the energy difference among the I, C, and S conformations is greatly reduced when the molecules are adsorbed on graphite.

An analysis of STM images suggests that the molecular S nanoarchitecture is stabilized by double hydrogen bonds between pyridine groups of neighboring molecules. These bonds are presented in Figure 3. Figure 5 reveals that when S molecules coexist with C, I, or L molecules, terpyridine groups of neighboring molecules are also always bound to each other through double N···H−C hydrogen bonds between pyridine groups. This suggests that this interaction is the dominant interaction driving the molecular self-assembly. This interaction should, however, be able to stabilize other structures based on I or C conformations of molecules, for example. STM shows that the quaterthiophene backbone surrounds a pyridine group of neighboring molecule in the S molecular nanoarchitecture. This maximizes intermolecular interactions between molecules in the S nanoarchitecture.

Molecular self-assembly is driven by the tendency of molecules to form the maximum number of interactions, as summarized by the close-packing principle. In that case, the S-molecule self-assembly is obviously more favorable than the I-molecule self-assembly because the contact area between neighboring molecules is larger. In addition, adsorbate molecules adsorb readily because they lower the surface free energy.[58] The packing density of the S-molecule nanoarchitecture is 20% denser than the packing density of the I-molecule nanoarchitecture. This also supports the fact that the S nanoarchitecture is more favorable than the I nanoarchitecture.

It should be noticed that the single-enantiomer structure (Figure 3) and the mixed-enantiomer structure (Figure 4) are stabilized by the same intermolecular interactions, i.e., a double hydrogen bond between pyridine groups and a similar intermolecular side-by-side contact area. However, the mixed-enantiomer structures were rarely observed, and these domains were very small. Self-assembled structures resulting from the self-assembly of the different molecular enantiomers are rarely observed. In the case of the 4T-bisterpy molecule, it seems that the molecular backbone conformation is at the origin of the less favorable arrangement of the two enantiomers, i.e., the backbone conformation in a two-enantiomer sequence (Figure 4) is less favorable than that in an S−S arrangement sequence (Figure 3).

CONCLUSIONS

In this paper we proved that a new bisterpyridine-quaterthiophene compound self-assembles into a hydrogen-bonded nanoarchitecture on graphite. The molecule does not adopt the lowest-energy conformation in this structure. The high conformational flexibility of this compound opens up new opportunities for tailoring molecular self-assembly and for engineering novel organic nanoarchitectures for applications in organic electronics.[36,59]

ASSOCIATED CONTENT

Supporting Information

The Supporting Information is available free of charge on the ACS Publications website at DOI: 10.1021/acs.langmuir.5b03949.

Synthesis pathway of the 4T-bisterpy compound, experimental details, full characterizations of intermediates and the final product, calculation details, and STM images of molecular self-assembly in additional solvents (PDF)

AUTHOR INFORMATION

Corresponding Author

*Phone: +33(0)169088019. Fax: +33(0)169088446. E-mail: fabien.silly@cea.fr.

Notes

The authors declare no competing financial interest.

ACKNOWLEDGMENTS

The research leading to these results has received funding from the European Research Council under the European Union's Seventh Framework Programme (FP7/2007-2013)/ERC grant agreement no. 259297.

REFERENCES

(1) Yang, L.; Tan, X.; Wang, Z.; Zhang, X. Supramolecular Polymers: Historical Development, Preparation, Characterization, and Functions. *Chem. Rev.* **2015**, *115*, 7196−7239.

(2) Seljamäe-Green, R. T.; Simpson, G. J.; Grillo, F.; Greenwood, J.; Francis, S. M.; Schaub, R.; Gano, J. E.; Früchtl, H. A.; Lacovig, P.; Baddeley, C. J. Formation of Bioinorganic Complexes by the Corrosive Adsorption of (S)-Proline on Ni/Au(111). *Langmuir* **2015**, *31*, 262−271.

(3) Skomski, D.; Jo, J.; Tempas, C. D.; Kim, S.; Lee, D.; Tait, S. L. High-Fidelity Self-Assembly of Crystalline and Parallel-Oriented Organic Thin Films by π-π Stacking from a Metal Surface. *Langmuir* **2014**, *30*, 10050−10056.

(4) Maeda, H. Supramolecular Chemistry of Pyrrole-Based π-Conjugated Molecules. *Bull. Chem. Soc. Jpn.* **2013**, *86*, 1359−1399.

(5) Liu, J.; Zhang, X.; Yan, H.; Wang, D.; Wang, J.; Pei, J.; Wan, L. Solvent-Controlled 2D Host-Guest (2,7,12-Trihexyloxytruxene/Coronene) Molecular Nanostructures at Organic Liquid/Solid Interface Investigated by Scanning Tunneling Microscopy. *Langmuir* **2010**, *26*, 8195−8200.

(6) Yue, J.-Y.; Liu, X.-H.; Sun, B.; Wang, D. The On-Surface Synthesis of Imine-Based Covalent Organic Frameworks with Non-Aromatic Linkage. *Chem. Commun.* **2015**, *51*, 14318−14321.

(7) Wu, R.; Yan, L.; Zhang, Y.; Ren, J.; Bao, D.; Zhang, H.; Wang, Y.; Du, S.; Huan, Q.; Gao, H.-J. Self-Assembled Patterns and Young's Modulus of Single-Layer Naphthalocyanine Molecules on Ag(111). *J. Phys. Chem. C* **2015**, *119*, 8208−8212.

(8) Uemura, S.; Aono, M.; Sakata, K.; Komatsu, T.; Kunitake, M. Thermodynamic Control of 2D Bicomponent Porous Networks of

DOI: 10.1021/acs.langmuir.5b03949
Langmuir 2015, 31, 13420−13425

Melamine and Melem: Diverse Hydrogen-Bonded Networks. *J. Phys. Chem. C* **2013**, *117*, 24815−24821.
(9) Rosei, F.; Schunack, M.; Naitoh, Y.; Jiang, P.; Gourdon, A.; Laegsgaard, E.; Stensgaard, I.; Joachim, C.; Besenbacher, F. Properties of Large Organic Molecules on Metal Surfaces. *Prog. Surf. Sci.* **2003**, *71*, 95−146.
(10) Yagai, S. Supramolecularly Engineered Functional π-Assemblies Based on Complementary Hydrogen-Bonding Interactions. *Bull. Chem. Soc. Jpn.* **2015**, *88*, 28−58.
(11) Yang, Y.; Wang, C. Hierarchical Construction of Self-Assembled Low-Dimensional Molecular Architectures Observed by Using Scanning Tunneling Microscopy. *Chem. Soc. Rev.* **2009**, *38*, 2576.
(12) Yan, H.; Zhu, L.; Li, D.; Zhang, Y.; Yi, Y.; Yang, Y.; Wei, Z.; Brédas, J.-L. Rationalization of the Selectivity in the Optimization of Processing Conditions for High-Performance Polymer Solar Cells Based on the Polymer Self-Assembly Ability. *J. Phys. Chem. C* **2014**, *118*, 29473−29481.
(13) Chen, L.-M.; Hong, Z.; Li, G.; Yang, Y. Recent Progress in Polymer Solar Cells: Manipulation of Polymer:Fullerene Morphology and the Formation of Efficient Inverted Polymer Solar Cells. *Adv. Mater.* **2009**, *21*, 1434−1449.
(14) Fitzner, R.; Elschner, C.; Weil, M.; Uhrich, C.; Körner, C.; Riede, M.; Leo, K.; Pfeiffer, M.; Reinold, E.; Mena-Osteritz, E.; Bäuerle, P. Interrelation between Crystal Packing and Small-Molecule Organic Solar Cell Performance. *Adv. Mater.* **2012**, *24*, 675−680.
(15) Hieulle, J.; Silly, F. Localized Intermolecular Electronic Coupling in Two-Dimensional Self-Assembled 3,4,9,10-perylenetetracarboxylic Diimide Nanoarchitectures. *J. Mater. Chem. C* **2013**, *1*, 4536−4539.
(16) Gusev, A. O.; Taleb, A.; Silly, F.; Charra, F.; Pileni, M.-P. Inhomogeneous Photon Emission Properties of Self-Assembled Metallic Nanocrystals. *Adv. Mater.* **2000**, *12*, 1583−1587.
(17) Yagai, S.; Goto, Y.; Lin, X.; Karatsu, T.; Kitamura, A.; Kuzuhara, D.; Yamada, H.; Kikkawa, Y.; Saeki, A.; Seki, S. Self-Organization of Hydrogen-Bonding Naphthalene Chromophores into J-type Nanorings and H-type Nanorods: Impact of Regioisomerism. *Angew. Chem., Int. Ed.* **2012**, *51*, 6643−6647.
(18) Mura, M.; Silly, F.; Burlakov, V.; Castell, M. R.; Briggs, G. A. D.; Kantorovich, L. N. Formation Mechanism for a Hybrid Supramolecular Network Involving Cooperative Interactions. *Phys. Rev. Lett.* **2012**, *108*, 176103.
(19) Barth, J. V.; Weckesser, J.; Cai, C.; Günter, P.; Bürgi, L.; Jeandupeux, O.; Kern, K. Building Supramolecular Nanostructures at Surfaces by Hydrogen Bonding. *Angew. Chem., Int. Ed.* **2000**, *39*, 1230−1234.
(20) Mura, M.; Silly, F.; Briggs, G. A. D.; Castell, M. R.; Kantorovich, L. N. H-Bonding Supramolecular Assemblies of PTCDI Molecules on the Au(111) Surface. *J. Phys. Chem. C* **2009**, *113*, 21840−21848.
(21) Barth, J. V. Molecular Architectonic on Metal Surfaces. *Annu. Rev. Phys. Chem.* **2007**, *58*, 375−407.
(22) Mura, M.; Sun, X.; Silly, F.; Jonkman, H. T.; Briggs, G. A. D.; Castell, M. R.; Kantorovich, L. N. Experimental and Theoretical Analysis of H-Bonded Supramolecular Assemblies of PTCDA Molecules. *Phys. Rev. B: Condens. Matter Mater. Phys.* **2010**, *81*, 195412.
(23) De Feyter, S.; De Schryver, F. C. Two-Dimensional Supramolecular Self-Assembly Probed by Scanning Tunneling Microscopy. *Chem. Soc. Rev.* **2003**, *32*, 139−150.
(24) Bonifazi, D.; Mohnani, S.; Llanes-Pallas, A. Supramolecular Chemistry at Interfaces: Molecular Recognition on Nanopatterned Porous Surfaces. *Chem. - Eur. J.* **2009**, *15*, 7004−7025.
(25) Silly, F.; Shaw, A. Q.; Castell, M. R.; Briggs, G. A. D.; Mura, M.; Martsinovich, N.; Kantorovich, L. Melamine Structures on the Au(111) Surface. *J. Phys. Chem. C* **2008**, *112*, 11476−11480.
(26) Xu, W.; Dong, M.; Gersen, H.; Rauls, E.; Vázquez-Campos, S.; Crego-Calama, M.; Reinhoudt, D. N.; Stensgaard, I.; Laegsgaard, E.; Linderoth, T. R.; Besenbacher, F. Cyanuric Acid and Melamine on Au(111): Structure and Energetics of Hydrogen-Bonded Networks. *Small* **2007**, *3*, 854−858.
(27) Sun, X.; Jonkman, H. T.; Silly, F. Tailoring Two-Dimensional PTCDA-melamine Self-Assembled Architectures at Room Temperature by Tuning Molecular Ratio. *Nanotechnology* **2010**, *21*, 165602.
(28) Hu, F.-Y.; Zhang, X.-M.; Wang, X.-C.; Wang, S.; Wang, H.-Q.; Duan, W.-B.; Zeng, Q.-D.; Wang, C. In Situ STM Investigation of Two-Dimensional Chiral Assemblies through Schiff-Base Condensation at a Liquid/Solid Interface. *ACS Appl. Mater. Interfaces* **2013**, *5*, 1583−1587.
(29) Suh, M. P.; Cheon, Y. E.; Lee, E. Y. Syntheses and Functions of Porous Metallosupramolecular Networks. *Coord. Chem. Rev.* **2008**, *252*, 1007−1026.
(30) Silly, F. Two-Dimensional 1,3,5-Tris(4-carboxyphenyl)benzene Self-Assembly at the 1-Phenyloctane/Graphite Interface Revisited. *J. Phys. Chem. C* **2012**, *116*, 10029−10032.
(31) Zhang, X.; Zeng, Q.; Wang, C. Molecular Templates and Nano-Reactors: Two-Dimensional Hydrogen Bonded Supramolecular Networks on Solid/Liquid Interfaces. *RSC Adv.* **2013**, *3*, 11351−11366.
(32) Wild, A.; Winter, A.; Schlütter, F.; Schubert, U. S. Advances in the Field of π-Conjugated 2,2′:6′,2″-terpyridines. *Chem. Soc. Rev.* **2011**, *40*, 1459−1511.
(33) Earmme, T.; Jenekhe, S. A. Solution-Processed, Alkali Metal-Salt-Doped, Electron-Transport Layers for High-Performance Phosphorescent Organic Light-Emitting Diodes. *Adv. Funct. Mater.* **2012**, *22*, 5126−5136.
(34) Roos, M.; Künzel, D.; Uhl, B.; Huang, H.-H.; Brandao Alves, O.; Hoster, H. E.; Gross, A.; Behm, R. J. Hierarchical Interactions and Their Influence upon the Adsorption of Organic Molecules on a Graphene Film. *J. Am. Chem. Soc.* **2011**, *133*, 9208−9211.
(35) Meier, C.; Landfester, K.; Ziener, U. Adsorbate-Substrate-Mediated Growth of Oligopyridine Monolayers at the Solid/Liquid Interface. *J. Phys. Chem. C* **2009**, *113*, 1507−1514.
(36) Mishra, A.; Ma, C.-Q.; Bäuerle, P. Functional Oligothiophenes: Molecular Design for Multidimensional Nanoarchitectures and Their Applications. *Chem. Rev.* **2009**, *109*, 1141−1276.
(37) Shen, Y.-T.; Guan, L.; Zhu, X.-Y.; Zeng, Q.-D.; Wang, C. Submolecular Observation of Photosensitive Macrocycles and Their Isomerization Effects on Host-Guest Network. *J. Am. Chem. Soc.* **2009**, *131*, 6174−6180.
(38) Mena-Osteritz, E.; Urdanpilleta, M.; El-Hosseiny, E.; Koslowski, B.; Ziemann, P.; Bäuerle, P. STM Study on the Self-Assembly of Oligothiophene-Based Organic Semiconductors. *Beilstein J. Nanotechnol.* **2011**, *2*, 802−808.
(39) Snegir, S. V.; Marchenko, A. A.; Yu, P.; Maurel, F.; Kapitanchuk, O. L.; Mazerat, S.; Lepeltier, M.; Léaustic, A.; Lacaze, E. STM Observation of Open- and Closed-Ring Forms of Functionalized Diarylethene Molecules Self-Assembled on a Au(111) Surface. *J. Phys. Chem. Lett.* **2011**, *2*, 2433−2436.
(40) Yokoyama, T.; Kurata, S.; Tanaka, S. Direct Identification of Conformational Isomers of Adsorbed Oligothiophene on Cu(100). *J. Phys. Chem. B* **2006**, *110*, 18130−18133.
(41) Jousselme, B.; Blanchard, P.; Gallego-Planas, N.; Delaunay, J.; Allain, M.; Richomme, P.; Levillain, E.; Roncali, J. Photomechanical Actuation and Manipulation of the Electronic Properties of Linear π-Conjugated Systems. *J. Am. Chem. Soc.* **2003**, *125*, 2888−2889.
(42) Brédas, J. L.; Street, G. B.; Thémans, B.; André, J. M. Organic polymers Based on Aromatic Rings (Polyparaphenylene, Polypyrrole, Polythiophene): Evolution of the Electronic Properties as a Function of the Torsion Angle Between Adjacent Rings. *J. Chem. Phys.* **1985**, *83*, 1323−1329.
(43) Hong, S. Y.; Song, J. M. Theoretical Study of Geometrical and Electronic Structures of Various Thiophene-Based Tricyclic Polymers. *J. Chem. Phys.* **1997**, *107*, 10607−10615.
(44) Jousselme, B.; Blanchard, P.; Allain, M.; Levillain, E.; Dias, M.; Roncali, J. Structural Control of the Electronic Properties of Photodynamic Azobenzene-Derivatized π-Conjugated Oligothiophenes. *J. Phys. Chem. A* **2006**, *110*, 3488−3494.
(45) Kikkawa, Y.; Ishitsuka, M.; Kashiwada, A.; Tsuzuki, S.; Hiratani, K. Bicomponent Blend-Directed Amplification of the Alkyl Chain Effect on the 2D Structures. *Chem. Commun.* **2014**, *50*, 13146−13149.

DOI: 10.1021/acs.langmuir.5b03949
Langmuir 2015, 31, 13420−13425

(46) Chen, T.; Yang, W.-H.; Wang, D.; Wan, L.-J. Globally Homochiral Assembly of Two-Dimensional Molecular Networks Triggered by Co-Absorbers. *Nat. Commun.* **2013**, *4*, 1389.
(47) Silly, F. Selecting Two-Dimensional Halogen-Halogen Bonded Self-Assembled 1,3,5-Tris(4-iodophenyl)benzene Porous Nanoarchitectures at the Solid-Liquid Interface. *J. Phys. Chem. C* **2013**, *117*, 20244−20249.
(48) Chin, Y.; Panduwinata, D.; Sintic, M.; Sum, T. J.; Hush, N. S.; Crossley, M. J.; Reimers, J. R. Atomic-Resolution Kinked Structure of an Alkylporphyrin on Highly Ordered Pyrolytic Graphite. *J. Phys. Chem. Lett.* **2011**, *2*, 62−66.
(49) Silly, F. A. Robust Method For Processing Scanning Probe Microscopy Images and Determining Nanoobject Position and Dimensions. *J. Microsc.* **2009**, *236*, 211−218.
(50) Turbiez, M.; Frére, P.; Allain, M.; Videlot, C.; Ackermann, J.; Roncali, J. Design of Organic Semiconductors: Tuning the Electronic Properties of π-Conjugated Oligothiophenes with the 3,4-Ethylenedioxythiophene (EDOT) Building Block. *Chem. - Eur. J.* **2005**, *11*, 3742−3752.
(51) Hoster, H. E.; Roos, M.; Breitruck, A.; Meier, C.; Tonigold, K.; Waldmann, T.; Ziener, U.; Landfester, K.; Behm, R. J. Structure Formation in Bis(terpyridine) Derivative Adlayers: Molecule-Substrate versus Molecule-Molecule Interactions. *Langmuir* **2007**, *23*, 11570−11579.
(52) Azumi, R.; Götz, G.; Debaerdemaeker, T.; Bäuerle, P. Coincidence of the Molecular Organization of β-Substituted Oligothiophenes in Two-Dimensional Layers and Three-Dimensional Crystals. *Chem. - Eur. J.* **2000**, *6*, 735−744.
(53) Müller, H.; Petersen, J.; Strohmaier, R.; Gompf, B.; Eisenmenger, W.; Vollmer, M. S.; Effenberger, F. Influence of polar Substituents on the Epitaxy of Oligothiophenes on Graphite: A Systematic STM Investigation. *Adv. Mater.* **1996**, *8*, 733−737.
(54) Abdel-Mottaleb, M. M. S.; Götz, G.; Kilickiran, P.; Bäuerle, P.; Mena-Osteritz, E. Influence of Halogen Substituents on the Self-Assembly of Oligothiophenes-A Combined STM and Theoretical Approach. *Langmuir* **2006**, *22*, 1443−1448.
(55) Stecher, R.; Gompf, B.; Münter, J. S. R.; Effenberger, F. Monolayers of Functionalized Oligothiophenes on Graphite-STM Investigation of the Influence of Intermolecular Interactions on the Epitaxy. *Adv. Mater.* **1999**, *11*, 927−931.
(56) Cicoira, F.; Miwa, J. A.; Melucci, M.; Barbarella, G.; Rosei, F. Ordered Assembly of α-Quinquethiophene on a Copper Oxide Nanotemplate. *Small* **2006**, *2*, 1366−1371.
(57) Yang, Z.-Y.; Zhang, H.-M.; Yan, C.-J.; Li, S.-S.; Yan, H.-J.; Song, W.-G.; Wan, L.-J. Scanning Tunneling Microscopy of the Formation, Transformation, and Property of Oligothiophene Self-Organizations on Graphite and Gold Surfaces. *Proc. Natl. Acad. Sci. U. S. A.* **2007**, *104*, 3707−3712.
(58) Love, J. C.; Estroff, L. A.; Kriebel, J. K.; Nuzzo, R. G.; Whitesides, G. M. Self-Assembled Monolayers of Thiolates on Metals as a Form of Nanotechnology. *Chem. Rev.* **2005**, *105*, 1103−1170.
(59) Perepichka, I. F.; Perepichka, D. F. *Handbook of Thiophene-Based Materials: Applications in Organic Electronics and Photonics*; John Wiley & Sons, 2009.

DOI: 10.1021/acs.langmuir.5b03949
Langmuir 2015, 31, 13420−13425